# The focal plane assembly for the Athena X-ray Integral Field Unit instrument

B. D. Jackson*[a], H. van Weers[b], J. van der Kuur[b], R. den Hartog[b], H. Akamatsu[b], A. Argan[c], S. R. Bandler[d], M. Barbera[e], D. Barret[f], M. P. Bruijn[b], J. A. Chervenak[d], J. Dercksen[b], F. Gatti[g], L. Gottardi[b], D. Haas[b], J.-W. den Herder[b], C. A. Kilbourne[d], M. Kiviranta[h], T. Lam-Trong[i], B.-J. van Leeuwen[b], C. Macculi[c], L. Piro[c], S. J. Smith[d]

[a] SRON Netherlands Institute for Space Research, Landleven 12, 9747 AD Groningen, The Netherlands; [b] SRON Netherlands Institute for Space Research, Sorbonnelaan 2, 3584 CA Utrecht, The Netherlands; [c] Istituto Nazionale di Astrofisica, Istituto di Astrofisica e Planetologia Spaziali Roma, Via del Fosso del Cavaliere 100, 00133 Roma, Italy; [d] NASA Goddard Space Flight Center, 662, Greenbelt, MD, USA 20771; [e] Università degli Studi di Palermo, Dipartimento di Fisica e Chimica, Via Archirafi 36, 90123 Palermo, Italy and Istituto Nazionale di Astrofisica, Osservatorio Astronomico di Palermo, Piazza del Parlamento 1, 90134 Palermo, Italy; [f] IRAP, L'Institut de Recherche en Astrophysique et Planetologie, Toulouse, France; [g] Università di Genova, Dipartimento di Fisica, Via Dodecaneso 33, 16146 Genova, Italy; [h] VTT Technical Research Centre of Finland, Tietotie 3, 02150 Espoo, Finland; [i] Centre National D'études Spatiales (CNES), Toulouse, France

## ABSTRACT

This paper summarizes a preliminary design concept for the focal plane assembly of the X-ray Integral Field Unit on the Athena spacecraft, an imaging microcalorimeter that will enable high spectral resolution imaging and point-source spectroscopy. The instrument's sensor array will be a ~ 3840-pixel transition edge sensor (TES) microcalorimeter array, with a frequency domain multiplexed SQUID readout system allowing this large-format sensor array to be operated within the thermal constraints of the instrument's cryogenic system. A second TES detector will be operated in close proximity to the sensor array to detect cosmic rays and secondary particles passing through the sensor array for off-line coincidence detection to identify and reject events caused by the in-orbit high-energy particle background. The detectors, operating at 55 mK, or less, will be thermally isolated from the instrument cryostat's 2 K stage, while shielding and filtering within the FPA will allow the instrument's sensitive sensor array to be operated in the expected environment during both on-ground testing and in-flight operation, including straylight from the cryostat environment, low-energy photons entering through the X-ray aperture, low-frequency magnetic fields, and high-frequency electric fields.

**Keywords:** X-ray microcalorimeter, transition edge sensor, cryogenic anti-coincidence detector, SQUID amplifier, frequency division multiplexing, Athena, X-IFU, focal plane assembly

## 1. INTRODUCTION

Athena, the Advanced Telescope for High-Energy Astrophysics,[1,2] is an X-ray telescope being developed to study the "Hot and Energetic Universe". Selected as the L2 mission in ESA's Cosmic Vision 2015-25 program, with a launch foreseen in 2028, Athena will combine an X-ray telescope with a 12-m focal length and an effective area of ~2 $m^2$ at 1 keV with two scientific instruments (the X-ray Integral Field Unit, X-IFU,[3] and the Wide Field Imager, WFI[4]) to study hot gas structures and supermassive black holes over cosmic time in the X-ray spectral range. The X-IFU is an imaging microcalorimeter incorporating a large-format superconducting Transition Edge Sensor (TES) detector array to enable high spectral-resolution imaging and bright point-source spectroscopy over 0.2-12 keV. A more complete description of the X-IFU science goals, requirements, and instrument concept can be found in Ref. 4.

*b.d.jackson@sron.nl; phone +31 50 363-8935; fax +31 50 363-4074; www.sron.nl

Space Telescopes and Instrumentation 2016: Ultraviolet to Gamma Ray, edited by Jan-Willem A. den Herder, Tadayuki Takahashi, Marshall Bautz, Proc. of SPIE Vol. 9905, 99052I · © 2016 SPIE · CCC code: 0277-786X/16/$18 · doi: 10.1117/12.2232544

## 2. THE FOCAL PLANE ASSEMBLY

The X-IFU instrument's combined requirements for high X-ray spectral resolution, moderately high point-source count-rate capability, and spectroscopic imaging over a large field-of-view drive the choice of a superconducting transition edge sensor (TES) microcalorimeter array as the instrument's sensor array, with frequency division multiplexed SQUID amplifiers reading out the low-impedance, low-noise TES thermometers. These detectors are packaged inside a focal plane assembly (FPA) that isolates the detectors, at a base temperature below 55 mK, from the 2 K cold stage of the X-IFU cryostat, with cooling of the FPA's cold stages via thermal straps from the instrument's sub-Kelvin cooler.

Besides thermal-mechanical isolation of the detector from the cryostat's 2 K cold stage, the FPA also includes electromagnetic shielding and filtering to ensure that the required sensitivity can be achieved within the electromagnetic environment of the instrument cryostat, including stray-light, low-energy photons entering the X-ray aperture, low-frequency magnetic fields, and high-frequency electric fields. A second TES detector (the cryogenic anti-coincidence detector, or CryoAC), is placed behind the sensor array to detect high-energy cosmic rays and secondary particles that pass through the sensor array, to allow non-X-ray events in the sensor array to be identified by their coincidence with events in the CryoAC, such that they can be flagged and rejected in the instrument's on-ground data processing pipeline.

Table 1 summarizes preliminary performance requirements for the X-IFU FPA derived from the instrument's science requirements[3] while Fig. 1 contains solid model drawing of the preliminary FPA design concept.

Table 1. Preliminary X-IFU FPA performance requirements.

| PROPERTY | REQUIREMENT |
|---|---|
| Energy range | 0.2-12 keV |
| Energy resolution* | $\delta E < 2.5$ eV FWHM for $E < 7$ keV, $E/\delta E > 2800$ for $E > 7$ keV (Req)<br>$\delta E < 1.5$ eV FWHM for $E < 7$ keV (Goal) |
| Count-rate** | 80% throughput with $\delta E \leq 2.2$ eV for a 1 mCrab point-source (Req)<br>80% throughput with $\delta E \leq 2.2$ eV for a 10 mCrab point-source (Goal)<br>$\leq 2$ cts/s/cm$^2$ in the telescope focal plane (extended source) |
| Quantum efficiency*** | > TBD% at 0.3 keV, > 92% at 1 keV, > 77% at 7 keV |
| Linearity | TBD |
| Array size (field of view) | 238 mm$^2$ (a 5' on the sky for a 12-m effective focal length telescope) |
| Non-X-ray background | $< 5\text{x}10^{-3}$ cts/s/cm$^2$/keV over 2-10 keV over 80% of the observing time, after on-ground processing of anti-coincidence data |

* These energy resolution figures correspond to the goals and requirements for the X-IFU instrument. The total FPA contribution to the 2.5 eV requirement should be ~ 2.2 eV in a root-sum-of-sum-of-squares noise budget.

** A "1 mCrab" point-source produces ~ 90 X-ray counts within the telescope's point spread function

*** Including the transmission of thermal filters in the FPA, plus the sensor array's absorber efficiency, geometrical fill-factor, and yield, but excluding losses in the filters in the X-IFU cryostat's aperture cylinder.

Key elements in the design concept seen in Fig. 1 that are discussed further in the sections that follow include:

- The 50 mK detector assembly, containing the sensor array, it's frequency division multiplexed SQUID readout electronics, the cryogenic anti-coincidence detector, and its (DC) SQUID amplifiers;
- A Niobium magnetic shield at 50 mK that can also provide shielding *vs.* radiated E-fields and stray-light, a mu-metal (e.g. Cryoperm) magnetic shield at 2 K, and an EMC-tight housing at 2 K;
- A 2 K electronics assembly that includes the sensor array's 2$^{nd}$ stage (booster) SQUID amplifiers and 2 K bias network, filtering of lines entering the FPA, and an interposer connector to the cryostat's 2-300 K cryo-harness;

- A two-layer thermal suspension system that isolates the detectors at 50 mK from the 2 K environment, with a 300 mK thermal intercept layer; and
- Thermometry, thermal straps, and a superconducting wiring harness linking the 50 mK and 2 K stages.

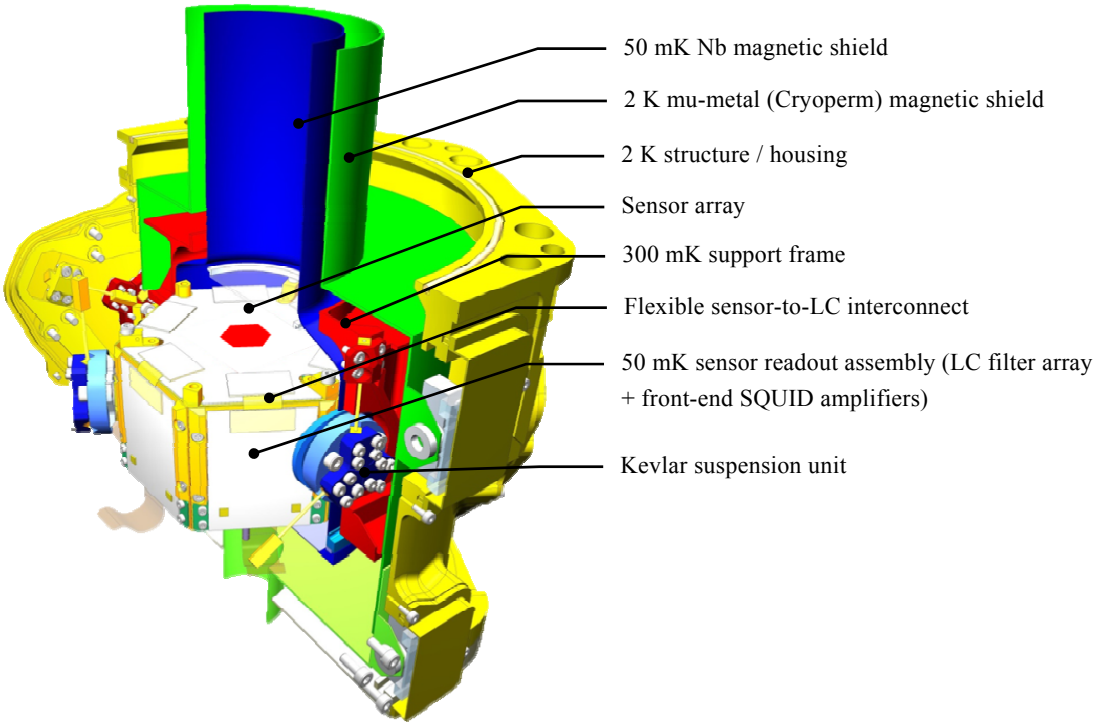


Figure 1. Preliminary design concept for the X-IFU focal plane assembly. (modified from Ref. 5)

## 3. SENSOR ARRAY AND MULTIPLEXED SQUID READOUT ELECTRONICS

The X-IFU FPA will incorporate a large-format TES microcalorimeter array to realize the instrument's need for sensitive and fast microcalorimeters that can be fabricated in kpixel-scale arrays with multiplexed readout electronics that can be operated within the tight constraints of the instrument's cryogenic cooling powers. In the preliminary design concept, this is realized using a uniform array of identical microcalorimeter pixels that simultaneously achieve the instrument's energy resolution, field-of-view, and point-source count-rate requirements in a single design. Based upon the expected operating temperature of the sensor array chip (< 55 mK) and heritage of past developments at GSFC, a MoAu TES with a superconducting transition temperature of ~ 90 mK will be used. The instrument's quantum efficiency, energy resolution, and count-rate requirements then drive a design with a Au/Bi X-ray absorber and a pixel pitch of ~ 249 μm, leading to a ~ 3840-pixel array to realize the required field-of-view. A hexagonal configuration of the square pixels allows efficient tiling on the sky for large-area raster maps while making efficient use of a round aperture in the FPA's magnetic shield baffle. A summary of key pixel and array characteristics is included in Ref. 6.

A major challenge in the development of the X-IFU FPA is the read-out of 3840 TES pixels within the available low-temperature (50 mK) cooling power. Superconducting SQUID amplifiers are naturally suited to the readout of TES microcalorimeters, combining low noise, low dissipation, and low input impedance, but with a typical dissipation of nW's per SQUID for a low-power, wide-band SQUID amplifier, the available cooling power 100's of nW implies a need to multiplex 10's of sensor array pixels per SQUID amplifier chain. Traditionally, three schemes have been developed for multiplexed readout of TES detectors with SQUID amplifiers: time division multiplexing (TDM),[7,8] code division multiplexing (CDM),[9,10] and frequency division multiplexing (FDM).[11,12] Systems using all three concepts have been demonstrated in the lab, and bolometric instruments using both TDM and FDM have been operated at ground-based

telescopes. Based on heritage of past IXO studies[13] and developments for the far-infrared bolometers for the SPICA-Safari instrument,[14,15] an FDM multixplexing scheme is baselined for X-IFU.

The baseline concept for the FDM-multiplexed SQUID readout of the X-IFU sensor array is depicted in Fig. 2. A comb of AC carriers in generated in the warm digital electronics and filtered in the cold using an array of superconducting low-loss LC filters (one filter per TES pixel),[16] such that each pixel is voltage-biased by a single AC carrier (to first order). The bias currents from the $N_{mux}$ pixels within a read-out channel are summed at the output of the LC filter array and pass to SQUID amplifiers at 50 mK and 2 K,[17,18] before leaving the cryostat for further amplification and processing in the warm electronics. Impedance transformers in the interconnects between the sensor and LC filter arrays match the ~ 1 mΩ set-point resistances of the TES thermometers to the ~ 2 μH inductors in the LC filters (chosen to minimize the filter surface area[14]), with the transformer ratio defining the effective inductance and resistance of the bias circuit as seen by the TES thermometer to control the pixels' speed in their set-point and the quality of the pixels' voltage bias.

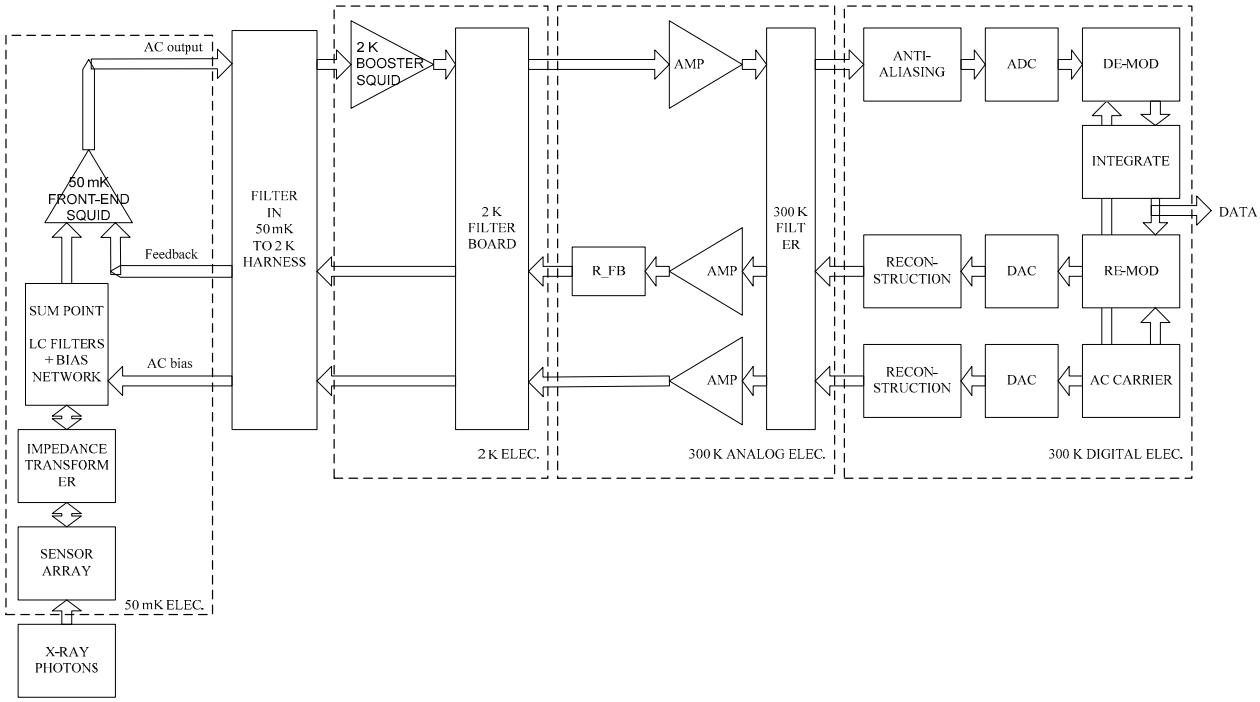


Figure 2. Block diagram of one 40-pixel channel of the frequency division multiplexed SQUID readout electronics that are baselined for readout of the FPA's sensor array, excluding SQUID bias supplies, the sensor array field coil, thermometry and thermal control, etc.. 96 readout channels will be operated in parallel to read out the instrument's full sensor array.

The limited dynamic range of a typical SQUID amplifier is overcome by applying baseband feedback (generated in the warm electronics) to suppress the AC carriers at the input to the first-stage (front-end) SQUID amplifier.[11,13] Besides accommodating the resulting post-feedback dynamic range in the sensor array's combined output signals, the SQUID amplifier chain should also provide sufficient gain to be operated with a ~ 1 nV/√Hz room-temperature amplifier, have an inter-stage bandwidth ≥ 8 MHz, a low input inductance (as seen from the LC filter array), and a differential output to the LNA. A two-stage amplifier chain, with a 50 mK front-end SQUID and a 2 K booster SQUID is used to meet this combination of requirements while also minimizing the heat-load on the instrument's 50 mK stage.

The achievable multiplexing factor in the preliminary system design is defined by a combination of the analog bandwidth of the SQUID amplifier chain and the cryostat's cable harness, the realizable density of AC carriers in frequency space, and the achievable dynamic range in the (to be developed) DACs that will generate the AC bias combs. These combine to give a preliminary multiplexing factor of 40, with carriers spaced by 100 kHz over 1-5 MHz.

More details can be found in Ref. 18, with the performance of prototype X-IFU pixels under MHz bias described in Ref. 19, and preliminary results of FDM multiplexing of prototype X-IFU pixels presented in Ref. 20.

## 4. NON-X-RAY BACKGROUND AND CRYOGENIC ANTI-COINCIDENCE DETECTOR

Beyond observations of bright point-sources, X-IFU will also observe low surface-brightness extended sources. For these low count-rate sources, events caused by high-energy cosmic rays passing through the sensor array (and secondary particles or photons that primary protons generate in the vicinity of the sensor array) can give a significant "non-X-ray background" in the instrument's X-ray spectra. Dedicated analyses are ongoing to determine the expected particle background inside the FPA,[21] and to simulate passive and active solutions to reduce the non-X-ray background, a combination of which are needed to realize the required background levels, including: a second detector array, a cryogenic anti-coincidence array or CryoAC,[22] located behind the sensor array to detect high-energy particles passing through the sensor array; applying a coating or liner material to suppress secondary particle and photons generated when high-energy particles passing through material in a direct line of sight of the sensor array; and heat-sinking the sensor array frame to suppress thermal pulses caused by cosmic ray impacts on the sensor array's bulk Si substrate.

The CryoAC detector[22] will be a few-pixel TES microcalorimeter with large-area absorbers that is designed to trigger on high-energy particles passing through the sensor array pixels, with a preliminary design concept that incorporates a 4-pixel TES microcalorimeter array with large (~1.15 $cm^2$) Si absorbers micromachined from a ~ 0.5 mm thick Si chip; a fast response (rise-time and thermal decay time); and a saturation energy of ~ 750 keV to minimize the dead-time after CryoAC events, given expected primary and secondary event rates and energies. The 4 CryoAC pixels are read-out with 4 DC SQUID amplifiers operating at ~ 55 mK.

## 5. DETECTOR PACKAGING AND SHIELDING

### 5.1 Cold detector and readout electronics assembly

The core of the FPA's 50 mK stage is the 50 mK detector and readout electronics assembly seen in Fig. 1. The detector assembly combines the large-format sensor array; six 50-mK sensor readout assemblies, each containing a 16-channel, 40 pixel/channel LC filter array and 16 front-end SQUID amplifiers; the CryoAC assembly mounted behind the sensor array and including both the CryoAC array and its SQUID amplifiers; a stiff structure; and housekeeping and auxiliary circuits, including thermometry and a magnetic field coil. The size of this assembly is driven by the surface area on the sensor array chip required for wiring fanout and electrical interconnects (resulting in a hexagon with a corner-to-corner dimension of 90-95 mm), and the surface area of 96x40 LC filters divided over the FPA's six side-panels.

The CryoAC array is mounted on a separate frame, together with its 4 DC SQUID amplifiers, to allow pre-integration testing independently of the sensor array, with a small gap between the CryoAC and sensor array chips to maximize the solid angle over which the CryoAC can detect cosmic rays passing through the sensor array pixels.[21,22]

A critical element of the 50 mK detector assembly is the electrical interconnect between the sensor array and the readout assemblies.[5] This connection must have a high wiring density (with ~ 640 pixels to be connected per side panel), low impedance (relative to the ~ 1 mΩ operating point resistance of a typical sensor pixel), realize a 90° bend between the sensor array and readout assembly, be robust vs. vibration, and (as a goal) allow mating / demating to facilitate testing and reworking. The preliminary concept for this interconnect employs a superconducting flex circuit terminated on both ends by bulk Si sections.[23] One termination will be used to implement a high-density bump-bond connection to the LC filter chip, while the second will be used to implement either a reworkable inductively coupled connection between transformer coil arrays on the interconnect and sensor chips or a second (not reworkable) high-density bump-bond.

### 5.2 FPA shielding and filtering architecture

As power detectors with bias powers of ~ 5 pW/pixel, noise levels of ~ 5 aW/√Hz, and superconducting thermistors that are sensitive to magnetic fields, X-IFU's microcalorimeters are very sensitive to electro-magnetic disturbances in their environment. Considering the expected environment of the X-IFU FPA, particular concerns in the preliminary design include quasi-static magnetic fields (*e.g.* variable stray fields from the cryostat's mechanical cryocoolers and sub-Kelvin cooler), conducted noise in the wiring harness leading from the warm electronics to the FPA, high-frequency radiated E-

fields that can couple to wiring in the vicinity of the TES's and/or directly to the microcalorimeters' X-ray absorbers, and photon noise from optical or infrared loading of the detector pixels by out-of-band radiation.

Out-of-band optical and infrared loading on the sensor array will be blocked by a stack of optical and thermal filters in the instrument cryostat's aperture cylinder and the FPA, in combination with the cryostat's thermal shields and the FPA's 2 K enclosure and 50 mK magnetic shield. Of the five optical/thermal filters included in the instrument's preliminary filter stack concept,[24] two are included in the FPA, at 2 K and 50 mK.

Based on past measurements of the magnetic field susceptibility of GSFC X-ray microcalorimeters,[25] preliminary requirements for the FPA's magnetic shielding are that the static field perpendicular to the sensor array should be less than 1 μT, with a uniformity of ~ 0.1 μT and a temporal stability of 5-10 pT. This will be realized by a combination of two shields in the FPA: a mu-metal (e.g. Cryoperm) shield at 2 K, and a superconducting Nb shield at 50 mK.[26] The mu-metal shield should give a field perpendicular to the sensor array of < 1 μT when the Nb shield passes through its superconducting transition temperature of ~ 9 K, while the combination of the mu-metal and Nb shields should suppresses temporal variability in the external field during sensor operation by a factor of a few $x10^5$.

A system-level study of the shielding of the X-IFU detectors from radiated E-fields and conducted noise in the cryostat structure is being performed in the instrument's Phase A study. Based upon early results from that study, three Faraday cages are assumed in the preliminary FPA design, at 300 K, 2 K, and 50 mK, with a primary layer of filtering at 300 K and higher-frequency filtering at cryogenic temperatures.

### 5.3 Thermal architecture

The FPA's thermal architecture isolates the detectors, at 50-55 mK, from the cryostat's 2 K cold stage. The FPA's thermal suspension should thus minimize the heat-load on the instrument's 50 mK cooler, have a high first eigenfrequency (≥ 300 Hz, to mechanically decouple the FPA from the structural resonances of the X-IFU instrument cryostat), realize a stable and predictable alignment of the sensor array with respect to the FPA's external mounting interface, and ensure survival of the expected launch loads. A 300 mK level provided by the instrument's sub-Kelvin provides a thermal intercept to minimize the heat-load on the 50 mK stage due to conduction through both the thermal suspension and wiring harnesses.

The preliminary thermal suspension concept that has been developed to address these requirements consists of a two-layer Kevlar suspension assembly in which each suspension layer is realized by an isostatic combination of three suspension units located concentrically around the 50 mK stage.[5] Each individual suspension unit is formed by a star of three Kevlar cords loaded in tension in a mechanical frame, with a pre-load applied to the Kevlar cords during assembly to ensure that all cords remain under tensile load both when at operating temperatures and under launch loads. A two-layer suspension is realized by stacking two suspensions, with the outer layer isolating a 300 mK support frame from 2 K and the inner layer isolating the 50 and 300 mK stages (part of the 300-50 mK suspension layer is visible in Fig. 1).

## 6. CONCLUSIONS

Located on the X-IFU cryostat's 2 K cold stage, the focal plane assembly will house X-IFU's two cryogenic detectors – a 3840-pixel TES microcalorimeter array that enables high-resolution spectroscopic imaging and (bright) point-source spectroscopy and a cryogenic anti-coincidence detector that detects high-energy cosmic rays and secondary particles and protons that pass through the sensor array, allowing coincidence of sensor array and CryoAC events to be used to remove non-X-ray background events that would otherwise degrade the instrument's sensitivity for weak sources. A frequency division multiplexed SQUID readout electronics system is used to operate 3840 TES microcalorimeter pixels in 96 channels of 40 pixels per channel, with critical components being low-loss superconducting LC filter arrays that split the 40-carrier AC bias combs so that each pixel is biased by a single carrier and a 2-stage SQUID amplifier chain that includes a low-dissipation front-end SQUID at 55 mK and a booster SQUID array at 2 K. Baseband feedback, making use of feedback signals generated in the warm readout electronics and coupled to the input of the front-end SQUID, is used to reduce the dynamic range requirement of the SQUID amplifier chain to allow the system's dynamic range requirement within the cryostat's 50 mK heat-lift. The 4-pixel CryoAC detector is operated using 4 DC SQUID channels.

With the instrument's two detector arrays operating at 55 mK, or less, the FPA contains an isostatic thermal suspension assembly that isolates the detectors from the 2 K environment of the cryostat's cold-stage, while multiple layers of

shielding and filtering are required to allow the 2.5 eV energy resolution requirement to be realized in practice. Within the FPA, this includes a mu-metal magnetic shield at 2 K and a superconducting Nb shield at 50 mK (which also serves as a Faraday cage for high-frequency E-fields), an EMI-tight 2 K housing (which is part of a larger 2 K Faraday cage X-IFU cryostat), thermal and optical filters in the X-ray apertures of the 50 mK Nb shield and the 2 K Faraday cage, and electrical filtering where signal lines pass enter the FPA's 2 K and 50 mK Faraday cages. A first layer of EMC shielding and filtering will be provided by the instrument cryostat's 300 K outer shell, while strong individual noise sources should be mitigated by local shielding at the source and/or operational planning.

## ACKNOWLEDGEMENTS

The authors would like to thank the team of scientists and engineers at SRON, INAF, University of Genoa / INFN, GSFC, VTT, NIST, and Stanford who are working to develop the X-IFU FPA and detector and the teams at CNES, IRAP, CEA-Grenoble, and CSIC who are leading the development of the X-IFU instrument and the instrument's cryostat in which the FPA will be integrated. This work was partially supported by ESAGSTP program contract 4000110555/14/NL/PA and CCN 1 to ESTEC contract 4200023035/10/NL/RA, and by the Netherlands Space Office PEP and PIPP programs.

## REFERENCES

[1] Nandra, K., Barret, D., Barcons, X., *et al.*, "The Hot and Energetic Universe: A White Paper presenting the science theme motivating the Athena+ mission," ArXiv e-prints (2013).
[2] Barcons, X., Nandra, K., Barret, D., den Herder, J.-W., Fabian, A. C., Piro, L., Watson, M. G., and the Athena Team, "Athena: the X-ray observatory to study the hot and energetic universe," J. of Physics Conference Series 610, 012008 (2015).
[3] Barret, D., Lam Trong, T., den Herder, J.-W. A., Piro, L., *et al.*, "The Athena X-ray Integral Field Unit," submitted to Proc. SPIE 9905 (2016).
[4] Meidinger, N., Eder, J., Eraerds, T., Nandra, K., Pietschner, D., Plattner, M., Rau, A., Strecker, R.., "The wide field imager instrument for Athena," submitted to Proc. SPIE 9905 (2016).
[5] van Weers, H. J., den Herder, J. W., Jackson, B. D., *et al.*, " TES-detector based focal plane assembly key-technology developments for ATHENA and SAFARI," Proc. SPIE 9144, 91445R, (2014).
[6] Smith, S. J., Adams, J. S., Bandler, S. R., *et al.*, "TES pixel parameter design of the microcalorimeter array for the x-ray integral field unit on ATHENA," submitted to Proc. SPIE 9905 (2016).
[7] Chervenak, J. A., Irwin, K. D., Grossman, E. N., Martinis, J. M., Reintsema, C. D., Huber, M. E., "Superconducting multiplexer for arrays of transition edge sensors," Appl. Phys. Lett. 74, 4043-4045 (1999).
[8] Doriese, W. B., Morgan, K. M., Bennett, D. A, *et al.*, "Developments in time-division multiplexing of X-ray transition-edge sensors," J. Low Temp. Phys. 184, 389-395 (2016).
[9] Irwin, K. D., Cho, H. M., Doriese, W. B., *et al.*, "Advanced code-division multiplexers for superconducting detector arrays," J. Low Temp. Phys. 167, 588-594 (2012).
[10] Fowler, J. W., Doriese, W. B., Hilton, G., Irwin, K., Schmidt, D., Stiehl, G., Swetz, D., Ullom, J. N., Vale, L. , "Optimization and analysis of code-division multiplexed TES microcalorimeters," J. Low Temp. Phys. 167, 713-720 (2012).
[11] van der Kuur, J., de Korte, P., de Groene, P., Baars, N., Lubbers, M., Kiviranta, M., "Implementation of frequency domain multiplexing in imaging arrays of microcalorimeters," Nucl. Instrum. Methods. A 520, 551-554 (2004).
[12] Dobbs, M. A., Lueker, M., Aird, K. A., *et al.*, "Frequency multiplexed superconducting quantum interference device readout of large bolometer arrays for cosmic microwave background measurements," R. Sci. Inst. 83(7), (2012).
[13] den Hartog, R., Beyer, J., Boersma, D., *et al.*, “Frequency domain multiplexed readout of TES detector arrays with baseband feedback,” IEEE Trans. Appl. Supercond., 21 (3), 289-293 (2011).

[14] van der Kuur, J., Beyer, J., Bruijn, M., *et al.*, " The SPICA-SAFARI TES Bolometer Readout: Developments Towards a Flight System," J. of Low Temp Physics 167 (5), 561-567 (2012).
[15] Jackson, B. D., de Korte, P. A. J., van der Kuur, J., *et al.*, " The SPICA-SAFARI Detector System: TES Detector Arrays With Frequency-Division Multiplexed SQUID Readout," IEEE Trans Terahertz Science and Technology *2*(1), 12-21 (2012).
[16] Bruijn, M. Gottardi, L. den Hartog, R., *et al.*, "Tailoring the high-q lc filter arrays for readout of kilo-pixel tes arrays in the spica-safari instrument," J. of Low Temp Phys 176, 421-425 (2014).
[17] Kiviranta, M., Gronberg, L., Beev, N., van der Kuur, J., "Some phenomena due to squid input properties when local feedback is present," J. of Physics: Conference Series 507(4), 042017 (2014).
[18] van der Kuur, J., Gottardi, L., Akamatsu, H., *et al.*, "Optimizing the multiplex factor of the frequency domain multiplexed readout of the TES-based microcalorimeter imaging array for the X-IFU instrument on the ATHENA x-ray observatory," submitted to Proc. SPIE 9905 (2016).
[19] Akamatsu, H., Gottardi, L., de Vries, C. P., *et al.*, "TES-based X-ray microcalorimeter performances under AC bias and FDM for Athena," J. of Low Temp. Phys. 184 (1), 436-442 (2016).
[20] Akamatsu, H., Gottardi, L., van der Kuur, J., *et al.*, "Development of the frequency domain multiplexing for the x-ray integral field unit (X-IFU) on the ATHENA," submitted to Proc. SPIE 9905 (2016).
[21] Lotti, S., Macculi, C., D'Andrea, M., *et al.*, "Updates on the background estimates for the X-IFU instrument onboard of the ATHENA mission," submitted to Proc. SPIE 9905 (2016).
[22] Macculi, C., Argan, A., D'Andrea, M., *et al.*, "The cryogenic anti-coincidence detector for ATHENA X-IFU: a program overview," submitted to Proc. SPIE 9905 (2016).
[23] Bruijn, M. P., van der Linden, A. J., Ridder, M. L., van Weers, H. J., "FDM readout assembly with flexible, superconducting connection to cryogenic kilo-pixel TES detectors," J. Low Temp. Physics 184 (1), 369-373 (2016).
[24] Barbera, M., Collura, A., Gatti, F., *et al.*, "Baseline design of the thermal blocking filters for the X-IFU detector on board ATHENA," SPIE Proc. 9144, 91445U (2014).
[25] Smith, S. J., Adams, J. S., Bailey, C. N., *et al.*, "Implications of weak-link behavior on the performance of Mo/Au bilayer transition-edge sensors," JAP 114, 074513 (2013).
[26] Bergen, A., van Weers, H. J., Bruineman, C., *et al.*, "Design and validation of a large-format TES-array magnetic shielding system for space applications," R. Sci. Inst., in press.